A Synchronization Metric for Meshed Networks of Pulse-Coupled Oscillators

Alexander Tyrrell and Gunther Auer
DOCOMO Euro-Labs
80687 Munich, Germany
lastname@docomolab-euro.com

Christian Bettstetter
University of Klagenfurt, Mobile Systems Group
9020 Klagenfurt, Austria
Firstname.Lastname@uni-klu.ac.at

ABSTRACT

Natural phenomena such as the synchronization of fireflies, interactions between neurons, and the formation of earthquakes are commonly described by the mathematical model of pulse-coupled oscillators. This article investigates the behavior of this model when oscillators form a meshed network, i.e. nodes are not directly coupled to all others. In order to characterize the synchronization process of populations of coupled oscillators we propose a metric that allows to characterize the level of local synchronization. We demonstrate the merits of the proposed local metric by means of two case studies that examine the effect of imperfections on the synchronization process, namely the presence of frequency drifts and propagation delays.

Keywords

synchronization, self-organization, biologically-inspired, pulse-coupled oscillators, delays, frequency drift

1. INTRODUCTION

Synchronization is a common ensemble behavior displayed by biological systems. Some striking examples include the synchronization of fireflies in South-East Asia where fireflies gather on trees at dawn and synchronize their blinking [4]; heart cells synchronizing so that the heart contracts appropriately [16]; the synchronous firing of neurons [9, 2]; and the formation of earthquakes [7]. A comprehensive overview of these phenomena is available in [19].

All these fascinating examples are governed by similar basic rules: each node, e.g. a firefly, a heart cell or a neuron, maintains a periodic function dictating when to pulse, and this function is adjusted when receiving pulses from other nodes. This oscillator model is known as *pulse-coupled oscillator* (PCO). Depending on intrinsic dynamics and on the rules defined for adjusting internal functions, different behaviors can be achieved.

To characterize the synchronization state in a population of coupled oscillators, Kuramoto introduced a synchronization metric in [11], which allows to study the effect of imperfections, such as frequency drift and noise [17]. The Kuramoto metric represents the degree of coherence in the network on a global scale, and therefore ignores the fact that nodes in self-organizing networks only interact locally with their neighbors. When nodes form a meshed network it is more meaningful to measure the synchronization state locally, only accounting for nodes that are directly connected. For instance, in wireless networks, local synchrony is more important than global synchrony with regards to packet transmissions, because the collision probability depends on local synchrony.

In this paper, a local synchronization metric targeted at meshed networks is presented, using elements from graph theory. The proposed metric is computed based on local information only, and enables individuals to *quantify* their local synchronization level.

To validate the proposed metric two case studies are conducted: the behavior of PCOs under imperfect clock conditions and the effect of propagation delays. Discrepancies in the frequency of internal oscillators are unavoidable in practice. It is shown that even in sparsely connected meshed networks and within certain limits on the coupling, PCOs are still able to synchronize. Propagation delays may cause instability to PCO synchronization [6]. This result is extended to meshed networks. The synchronization metric allows to characterize and quantify the transition from the initial unordered state to the stable synchronized state in the presence of delays.

This paper is structured as follows. Section 2 presents the PCO model describing firefly synchronization and some of its applications to neural networks and wireless networks. Section 3 introduces a measure for local synchrony, and examines its behavior under two illustrative network topologies. Finally Sections 4 and 5 apply the local metric to characterize the behavior of PCOs in the presence of frequency drift and propagation delays, respectively.

2. BIOLOGICALLY-INSPIRED SYNCHRONIZATION

The theory of PCOs describes entities that mutually interact at discrete time instances via infinitely short pulses. The first part of this section reviews PCO synchronization and introduces the underlying rules leading to in-phase synchronization, i.e. all oscillators pulse simultaneously. Thanks to its simple set of local rules, the PCO model has been considered in different fields. Some of these applications are summarized in the second part.

Bionetics '08, November 25-28, 2008, Hyogo, Japan

2.1 Pulse-Coupled Oscillator Synchronization

A system of N pulse-coupled oscillators is considered, and each node n, n=1, ..., N in the system is described by its phase variable ϕ_n, which determines when a pulse is emitted. The evolution of ϕ_n over time depends on the node's internal dynamics and on interactions with other nodes.

As long as no pulse is perceived, a node behaves as an uncoupled oscillator. Its phase variable ϕ_n grows linearly over time with a given rate:

$$\frac{\mathrm{d}\phi_n}{\mathrm{d}t} = \frac{1}{T} \,. \tag{1}$$

Whenever ϕ_n=1 at reference instant t=τ_n, the node *fires*: it emits an infinitely short pulse, and the phase variable is reset to 0, increases again linearly, and so on. Thus, if the oscillator is uncoupled or it does not receive any pulse between two firing instants, it fires with constant period T.

Based on this phase function, we define an internal clock c_n for node n:

$$c_n = \exp\left(\mathrm{j}\, 2\pi\, \phi_n\right) \,. \tag{2}$$

For an uncoupled node, the internal clock c_n rotates around the unit circle at constant speed $1/T$, and passes through the firing instant c_n=1 every T seconds.

Synchronization rules. When a node m fires at instant t=τ_m and if nodes n and m are coupled, the phase variable ϕ_n is adjusted upon reception of the pulse from m. When receiving such a pulse, node n instantly increments its phase, depending on its current internal state $\phi_n(\tau_m)$. The total system behavior is described by:

$$\phi_m(\tau_m) = 1 \Rightarrow \left\{ \begin{array}{l} \phi_m(\tau_m^+) = 0 \\ \phi_n(\tau_m^+) = \phi_n(\tau_m) + \Delta\phi\left(\phi_n(\tau_m)\right), \forall n \in \mathcal{N}_m \end{array} \right. \tag{3}$$

where τ_m^+=τ_m+dt, and $\mathcal{N}_m$ denotes the set of nodes coupled to m. The increment function $\Delta\phi\left(\phi_n\right)$ is called phase response curve (PRC).

In [15] conditions on the PRC to reach synchrony for arbitrary initial time offsets are identified. A simple PRC leading to synchrony is the piecewise linear function

$$\phi_n + \Delta\phi\left(\phi_n\right) = \min\left(\alpha \cdot \phi_n + \beta, 1\right) \,. \tag{4}$$

The terms α and β are the coupling parameters: α is the slope and β is the initial value of the PRC. Assuming that each node maintains the same PRC, if $\alpha > 1$ and $0 < \beta < 1$, a set of nodes always synchronizes independently of the initial conditions. The time to synchrony is inversely proportional to α. Figure 1 plots an example of the PRC (4) for α=1.3 and β=0.01.

Synchronization process. A key feature in the synchronization of PCOs is that, over time, nodes cluster into groups of oscillators. This phenomenon is referred to as *absorption*, and occurs when the pulse of a firing node forces other nodes to exceed their firing threshold, causing them to fire at the same instant. As nodes have the same internal dynamics, in a fully-meshed network where all nodes are mutually coupled, absorptions are permanent. Mirollo and Strogatz show that the set of initial conditions that never leads to any absorption has a Lebesgue measure of zero [15]. Therefore nodes following the PCO rules always synchronize from any initial condition; nodes first gather into groups that gradually absorb one another, eventually forming one synchronized group. In [12] Lucarelli and Wang extended the demonstration to meshed networks where nodes are locally coupled, and absorptions are not permanent.

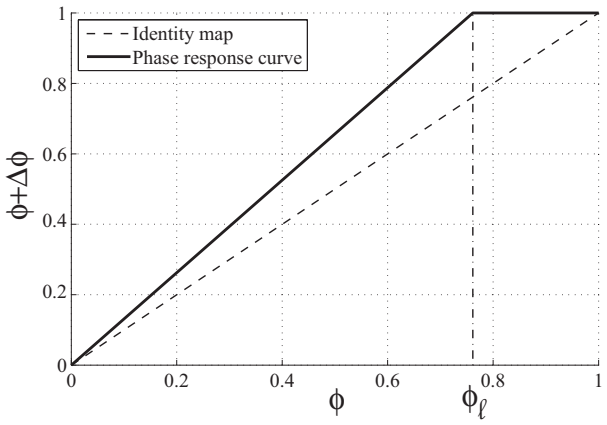

Figure 1: Phase response curve for α=1.3 and β=0.01.

2.2 Applications of PCO Dynamics

The mathematical model of PCOs provides simple rules leading to synchronization, and has been applied to different fields, integrating different constraints.

The application of PCOs to wireless systems is particularly attractive, especially in ad hoc networks, as it enables networks to synchronize in a distributed manner. Various implementations and adaptations to wireless networks have been considered, and some include:

- utilizing the characteristic pulse of Ultra Wide Band (UWB) radio to imitate the PCO synchronization principle [8];
- considering long synchronization sequences instead of pulses, and appropriately delaying interactions so that the accuracy is upper bounded by propagation delays [20];
- placing the synchronization unit on the MAC layer, and performing synchronization through the exchange of a low-level timestamp [21];
- achieving a round-robin schedule in a decentralized manner by modifying the PCO model so that nodes fire one after the other with a constant offset [5].

Another interesting application of PCO dynamics is the study of neural networks. Each neuron is modeled as an oscillator that emits electrical impulses periodically, and adjusts its emission instant when receiving impulses from other neurons. The phase model for PCOs enabled Izhikevitch [9] to study neural systems and to show possible behaviors, e.g. synchronization if neurons have roughly the same internal frequency, or oscillatory associative memory behavior under certain coupling assumptions.

PCO dynamics have also been applied to design a computationally efficient image processing algorithm. In [18] the PCO model is applied to perform image clustering. A coupling function different to (4) is defined that organizes a

population of PCOs into clusters: within each cluster oscillators fire synchronously, while clusters themselves fire with a constant phase difference.

3. SYNCHRONIZATION METRIC

The objective of a synchronization metric is to identify whether a network is synchronized and to quantify the state of the system. When all nodes are synchronized in-phase, i.e. they all fire at the same instant, the metric should be equal to 1. When the system is in disorder, i.e. firing instants are randomly distributed within $[0, T]$, the metric should approach 0.

This section details an global metric derived by Kuramoto [11]. Then a new metric targetted at locally coupled oscillators is presented, and applied to two particular network topologies to motivate its behavior.

3.1 Global Synchronization

The Kuramoto model introduces the *mean field* of phases, defined as [11]:

$$r\, \exp\left(\mathrm{j}\, 2\pi\, \bar{\phi}\right) = \frac{1}{N} \sum_{n=1}^{N} \exp\left(\mathrm{j}\, 2\pi\, \phi_n\right) = \frac{1}{N} \sum_{n=1}^{N} c_n \qquad (5)$$

where r is the Kuramoto synchronization index, and $\bar{\phi} \in [0, 1]$ is the mean phase of all N oscillators.

The mean field r is an indicator of the coherence due to synchronization in the network. If all phases are equal, the complex exponentials in (5) add up constructively and r=1. If phases are uniformly distributed in $[0, 1]$, then $r \to 0$.

The Kuramoto metric for N=2 nodes evolves according to:

$$r = \sqrt{\tfrac{1}{2}\left(1 - \cos\left(2\pi(\phi_m - \phi_n)\right)\right)}\ . \qquad (6)$$

The Kuramoto metric is not specific to any oscillator model, and can be applied to the PCO model presented in Section 2.1. As an example, Figure 2 plots the evolution of N=20 phases following the simple rules of (1) and (3), and the corresponding Kuramoto synchronization index r.

From Figure 2 the synchronization index starts with a value close to r=0, and jumps abruptly when a node fires, this jump being proportional to the number of firing nodes. After three periods, two groups of oscillators have formed, at which point the metric remains close to r=0. Then the metric gradually converges to r=1, and synchronization is reached after six periods. The Kuramoto model (2) characterizes the state of N nodes with a single number, and thus captures the degree of coherence in a simpler manner than the evolution of phases.

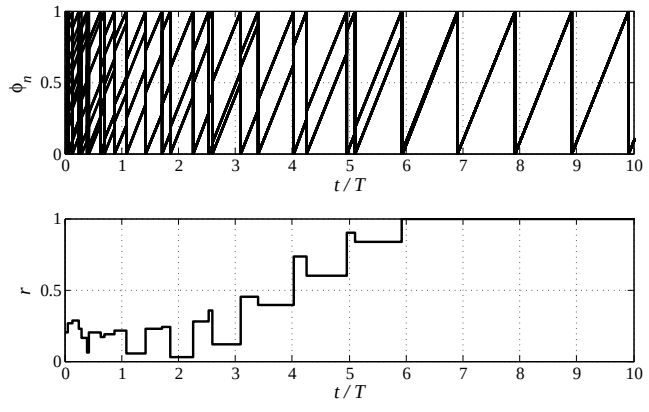

Figure 2: Evolution of phases ϕ_n over time and the corresponding Kuramoto synchronization index r.

3.2 Local Synchronization

The Kuramoto index (5) is defined for the whole network. In this section we define a metric targeted at meshed networks where nodes interact locally, so that the synchronization state of a node with regards to its neighbors can be quantified. Before presenting the metric, some preliminaries from graph theory are summarized, which establishes a measure for the connectivity of a given network.

3.2.1 Meshed Network

The topology of a meshed network is modeled as a graph $\mathcal{G}$ consisting of a set of N nodes denoted by $\mathcal{V}$ and a set of links denoted by $\mathcal{E}$. Two nodes that have a joint link are called neighbors. The set of neighbors of node n is defined as $\mathcal{N}_n = \{m : (n, m) \in \mathcal{E}\}$. The number of neighbors of node n, $|\mathcal{N}_n|$, is the *degree* of the node. If all node pairs are connected by a link, the degree of each node is $N-1$, and the network is said to be *fully-meshed*.

The degree matrix of $\mathcal{G}$, denoted by $\mathbf{\Delta}(\mathcal{G})$, is a diagonal matrix whose elements are equal to the degree of node n on the n-th diagonal element and 0 elsewhere. The adjency matrix of $\mathcal{G}$ is denoted by $\mathbf{A}(\mathcal{G})$, and its elements on line n and column m are equal to a_{nm}=1 if nodes n and m are connected and a_{nm}=0 otherwise. For an undirected graph, $\mathbf{A}(\mathcal{G}) = \mathbf{A}^T(\mathcal{G})$, where $[.]^{\mathrm{T}}$ denotes the transpose operator.

The Laplacian matrix [1] is equal to:

$$\mathbf{L}(\mathcal{G}) = \mathbf{\Delta}(\mathcal{G}) - \mathbf{A}(\mathcal{G})\ . \qquad (7)$$

The spectrum of $\mathbf{L}(\mathcal{G})$ characterizes topological properties of $\mathcal{G}$ [1]. The second smallest eigenvalue of $\mathbf{L}(\mathcal{G})$ is denoted by κ, and is called algebraic connectivity. If the network is connected, i.e. there exists a path between any two nodes, then $\kappa > 0$. If the network is fully-meshed, then $\kappa = N$. The algebraic connectivity is an adequate measure of the network topology when studying synchronization [14].

3.2.2 Local Metric

The state of a node is conveniently represented by its clock (2), in terms of the complex exponential of its phase. The proposed local synchronization metric for node n is defined as the normalized sum of pairwise differences of local clocks:

$$r_n = 1 - \frac{1}{|\mathcal{N}_n|} \left| \sum_{m \in \mathcal{N}_n} (c_n - c_m) \right|\ . \qquad (8)$$

The local metric is defined in the interval $r_n \in [-1, 1]$.

It is instructive to study the local metric by the evolution of the clock difference $c_n - c_m$ in the complex plane. Figure 3 shows the two clock vectors c_n and c_m and their resulting difference $c_n - c_m$, which constitutes one element of the sum in (8). In Figure 3 the phase of node n is equal to ϕ_n=0. The set of possible resulting clock differences $c_n - c_m$ describes a circle, which is plotted with a dashed line in Figure 3.

If node n is synchronized with all its neighbors, then $c_n = c_m$, $\forall m \in \mathcal{N}_n$ so that their difference is equal to 0, and the local metric yields r_n=1.

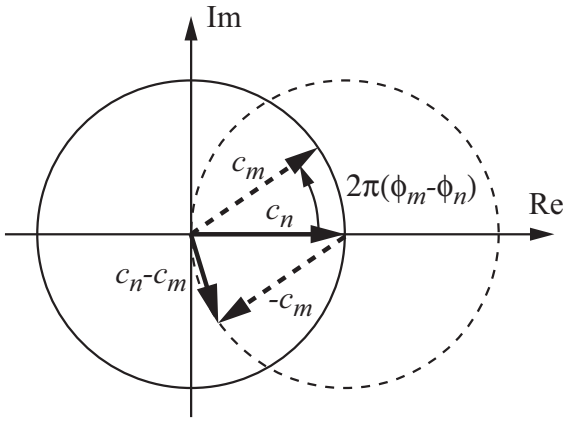

Figure 3: Geometric representation of two clock vectors c_n and c_m and their resulting difference $c_n - c_m$.

Two interesting special cases also result in r_n=0. If neighboring nodes in $\mathcal{N}_n$ form two groups of equal size and are anti-phase synchronized, i.e. the firing instants of each group are delayed by $T/2$, then the pairwise difference in the sum over m with c_n in (8) gives 0 in half the sum and 2 in the other half, resulting in a total metric of r_n=0. The metric also yields r_n=0 when phases of neighboring nodes are equally spaced in $[0, 1]$. In this case, the pairwise difference with the clock of node n cancel each other, so that the normalized sum in (8) becomes 1, which results in r_n=0.

The local metric gives r_n=−1 when two anti-phase synchronized groups form, one composed of node n only and all its neighbors forming the second group. Then c_n=$-c_m$, $\forall m \in \mathcal{N}_n$, so that the magnitude of the clock difference becomes $|c_n - c_m|$=2, which yields r_n=−1. Therefore r_n is an appropriate metric for characterizing the local synchronization state.

The resulting metric for N=2 nodes is r_n=1−$|c_n - c_m|$, which yields, using the law of cosines

$$r_n = 1 - \sqrt{2\big(1 - \cos(2\pi(\phi_m - \phi_n))\big)}\ . \tag{9}$$

Figure 4 compares the Kuramoto global metric (6) and the proposed local metric (9) as the phase difference $\phi_m - \phi_n$ varies in a system of N=2 nodes. From Figure 4 the Kuramoto metric is less penalizing against small phase differences. On the other hand, the proposed local metric decreases rapidly as the phase difference increases. For instance, when $\phi_m - \phi_n$=0.1, the local metric yields $r_n \approx 0.4$, whereas the global metric yields $r_n \approx 0.95$. Around the maximum phase difference at $\phi_m - \phi_n$=0.5, the slope of the global metric is discontinuous, whereas the local metric has a smooth trajectory. Therefore the local metric pronounces small phase changes but hardly varies when the phase difference is maximal. We believe that these are desirable properties of the proposed metric.

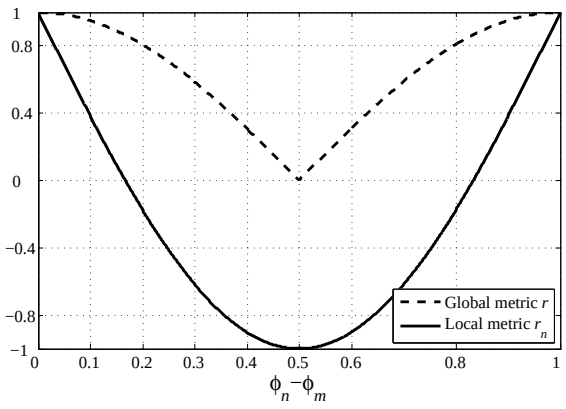

Figure 4: Resulting global and local metrics as the phase difference $\phi_m - \phi_n$ varies in a system of 2 nodes.

A further difference between the proposed metric and the Kuramoto metric is that the former is exclusively computed based on local information, as the sum in (8) depends only on neighboring clocks. This is particularly useful when applying the metric to self-organizing networks where only local information is available.

The proposed metric can be conveniently reformulated as a function of the degree and Laplacian matrices. Let $\mathbf{C}$ be defined as the vector of all internal clocks $\mathbf{C} = [c_1 \dots c_N]^{\mathrm{T}}$. Then the local synchronization metric can be written as:

$$\mathbf{r} = 1 - \left|(\mathbf{\Delta}(\mathcal{G}))^{-1} \cdot \mathbf{L}(\mathcal{G}) \cdot \mathbf{C}\right| \tag{10}$$

with $\mathbf{r} = [r_1, \dots, r_N]^{\mathrm{T}}$.

3.2.3 Case Study: Two Interconnected Clusters

A benefit of the local metric can be observed when applying it to the network topology shown in Figure 5. In this network, nodes within the same cluster can directly communicate, while the two clusters are interconnected by only one pair of nodes. The algebraic connectivity of this network is κ=8.91.

Figure 6 presents the evolution of the global and local metrics for this particular topology. During the first three periods, each cluster synchronizes almost independently, and the local metric increases very rapidly to a value close to r_n=1, whereas the global metric decreases to r=0.15. This reflects the fact that nodes synchronize first with their direct neighbors. After this initial phase, the two clusters mutually synchronize, and global synchronization is reached after seven periods. During this time, the local metric does not reach r_n=1, because one neighbor of n is connected to the other cluster, which perturbs the synchronization index r_n.

3.2.4 Case Study: Ring of Oscillators

The *diameter* of the network is a common measure to describe a given topology; it is equal to the maximum number of links on the shortest path between any node pairs. To compare the behavior of the global Kuramoto metric and

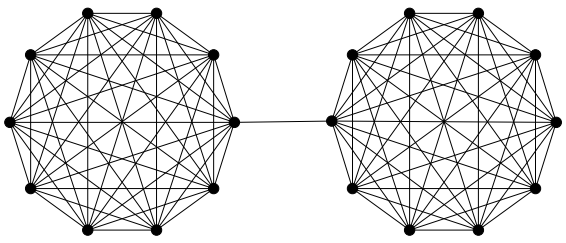

Figure 5: Two fully-meshed networks of 10 nodes interconnected by one link.

the proposed metric, N oscillators form a ring and communicate directly with the two nodes that have the smallest physical distance. The diameter of such a topology is equal to $N/2$ when N is even and to $(N-1)/2$ when N is odd. Figure 7 plots the evolution of the average global and local metrics over time for $1,000$ sets of initial conditions. The coupling parameters are set to α=1.2 and β=0.01, and there is a constant interaction delay of $0.01\,T$ between two connected nodes.

Increasing the network diameter impacts heavily the global metric. For N=20, the metric converges to a value close to 1, which indicates that the whole network has approximately the same phase value. As the diameter increases, the global metric oscillates before settling to a decreasing value as N increases. This oscillating behavior is due to the constant delay between nodes [3]. On the other hand, the local metric does not change as N varies, which confirms that nodes are synchronized on a local scale.

4. FREQUENCY DRIFT

A common question in network synchronization is to determine the robustness of a scheme with regards to frequency drifts. In (1) the phases of all nodes evolve with a constant rate $1/T$, but in practice, two oscillators are in general not identical, and their internal frequency is distributed around some nominal value.

In the presence of frequency drift γ_n, the internal clock rate (1) of node n becomes:

$$\frac{\mathrm{d}\phi_n}{\mathrm{d}t} = \frac{1+\gamma_n}{T}\ . \tag{11}$$

We assume that γ_n is uniformly distributed in $[-\gamma_{\max}, \gamma_{\max}]$. Thus the natural periods of uncoupled oscillators are distributed between $T_{\min}$=$T/(1+\gamma_{\max})$ and $T_{\max}$=$T/(1-\gamma_{\max})$.

Phase increments of the phase response curve (3) are always strictly positive (see Figure 1). Therefore nodes always shorten their period and advance their next firing instant, and thus attempt to catch up with a received pulse. In the presence of frequency drifts, nodes thus tend to catch up with the quickest oscillator, i.e. the node with the shortest natural period $T_{\min}$.

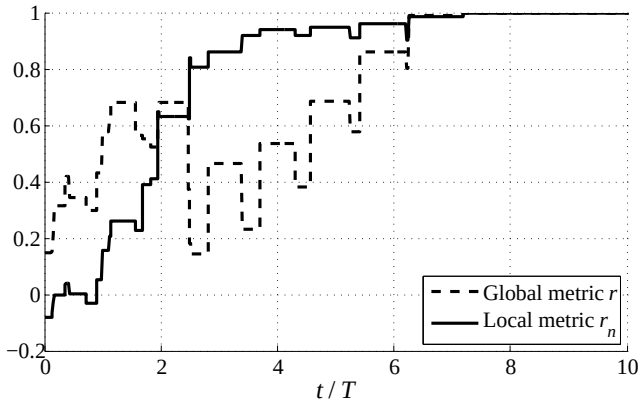

Figure 6: Evolution over time of the global and local synchronization metrics for the two interconnected fully-meshed networks.

If the frequency drift γ_n is too severe, some nodes are not able to catch up with the quickest oscillator. To establish the frequency drift limit, Figure 1 plots the phase limit ϕ_ℓ: if the phase of a node is superior to ϕ_ℓ when receiving a pulse, the node fires immediatly. Thus nodes whose phase is the interval $[\phi_\ell, 1]$ are absorbed by the received pulse. The phase limit for absorption yields:

$$\phi_\ell = \frac{1-\beta}{\alpha}\ . \tag{12}$$

All nodes are absorbed by the pulse of the fastest oscillator if their phase is in the interval $[\phi_\ell, 1]$. This imposes a condition on the slowest oscillator, which should have a phase $\phi_{\min} \geq \phi_\ell$ when the quickest oscillator fires. This minimum phase is $\phi_{\min} = T_{\min}/T_{\max} = (1-\gamma_{\max})/(1+\gamma_{\max})$, which gives the following condition for the maximum clock drift:

$$\gamma_{\max} \leq \frac{1-\phi_\ell}{1+\phi_\ell}\ . \tag{13}$$

The absorption by the quickest node repeats itself periodically, and re-aligns all phases every period. Therefore, once nodes have synchronized, the synchronization metric stays equal to one as long as condition (13) is met. To verify that this condition is valid in meshed networks, Figure 8 plots the evolution over time of the mean local synchroniza-

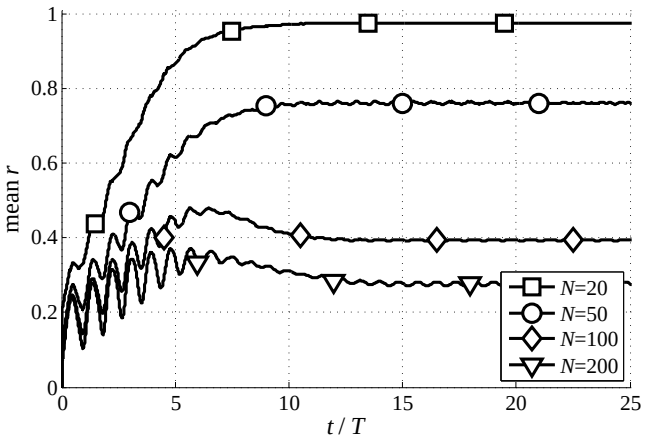

(a) Global metric

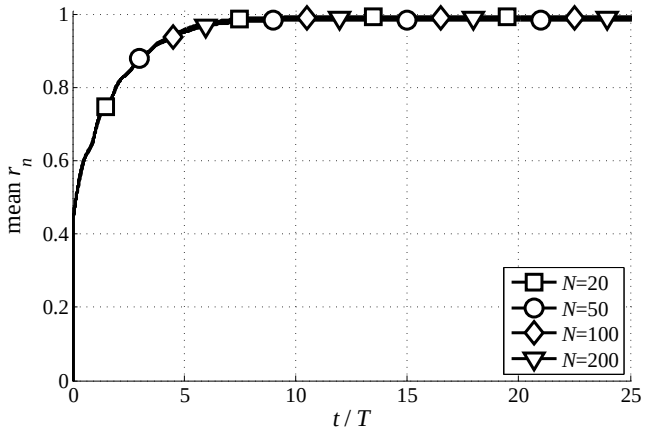

(b) Local metric

Figure 7: Evolution over time of the mean global and local metrics in a ring of N oscillators.

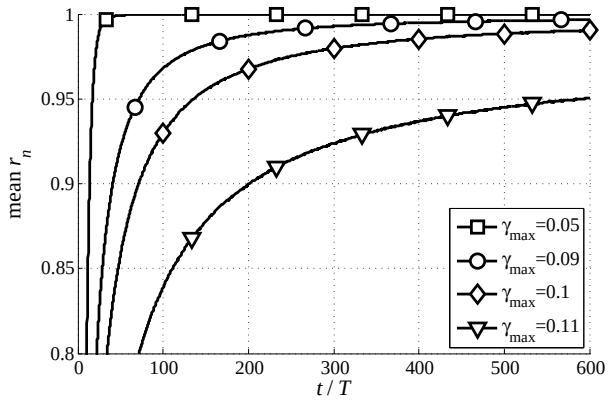

Figure 8: Evolution over time of the mean local synchronization metric in the presence of frequency drift.

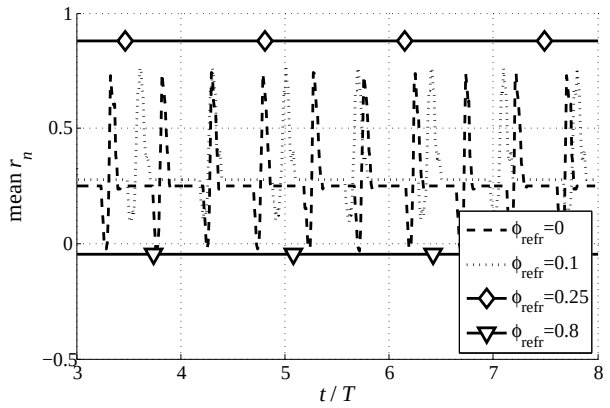

Figure 9: Example of the time evolution of the synchronization index for different refractory durations.

tion metric for several values of $\gamma_{\max}$ obtained in networks of N=25 nodes with an algebraic connectivity of κ=0.03. Under the condition α=1.2 and β=0.01, the maximum clock drift from (13) is equal to $\gamma_{\max}\approx$0.10. In Figure 8 as long as the drift is below this threshold, nodes are still able to synchronize although the time to synchrony augments as the drift increases. When the drift threshold is exceeded at $\gamma_{\max}$=0.11, a large gap in the synchronization metric is observed. Nevertheless the system is more ordered than in the initial unordered state, because only a few nodes are unable to follow the quickest node.

5. PROPAGATION DELAYS

When applying the PCO model to wireless networks, propagation delays delay the coupling between nodes. It was shown in [6] that coupling delays may lead to instability. By the introduction of a refractory period where phase adjustments are not permitted, stability is regained. In this section unstable synchronization states and the effect of a refractory period are characterized by the local synchronization metric.

5.1 Refractory Period

Introducing coupling delays in a system of PCOs may lead to an unstable system that is unable to synchronize [6]. To regain stability, a refractory period after sending a pulse is introduced [13]. During refractory, i.e. when $\phi_n<\phi_{\text{refr}}$, no phase increment is possible, so that pulses from neighboring nodes are not acknowledged.

In [13], it was shown for two nodes that the system remains stable if "echos" are not acknowledged, which is ensured by setting the refractory period to

$$\phi_{\text{refr}} > 2\,\frac{\nu}{T} \tag{14}$$

where ν accounts for the propagation delay between the two considered nodes. Under these conditions and if $\phi_{\text{refr}}<0.5$ [10], the system converges to a stable state where firing instants are shifted by ν [13].

5.2 Delays in Meshed Networks

Determining the stable state achieved by a system of PCOs in the presence of coupling delays is a difficult task. In a fully-meshed network where all nodes are coupled directly to all others, the two node case can be generalized as follows: if the refractory duration is at least equal to twice the maximum propagation delay, the first firing node forces its delayed firing instant onto other nodes, because it discards their echos. Echos are discarded if ϕ_{refr}, the refractory duration common to all nodes, satisfies the following condition:

$$\phi_{\text{refr}} > 2\,\max_{n,m}\frac{\nu_{nm}}{T} \tag{15}$$

where ν_{nm} accounts for the propagation delay between node n and its neighbors m. Therefore, in a fully-meshed network, firing instants are spread within an interval $[\tau_1, \tau_1+\nu_{\max}]$ where τ_1 is the firing instant of the first firing node and $\nu_{\max}$ is the maximum propagation delay with this node.

In a meshed network, the stable state is not as clear, because the first firing node does not directly influence all other nodes. To the best of our knowledge, the impact of propagation delays in this case is an unsolved problem. We thus apply the local synchronization metric to examine whether the stability condition (15) is valid. As an example, Figure 9 plots the evolution of the metric for several values of the refractory duration in a network of N=12 nodes with connectivity κ=6 and a maximum propagation delay of $0.1\,T$.

The synchronization metric in Figure 9 displays different behaviors depending on the duration of the refractory period. If ϕ_{refr} is too short and (15) is not met locally, then r_n oscillates, which corresponds to an unstable state as phases never align. If the refractory period is too large, i.e. $\phi_{\text{refr}}>0.5$, nodes are not able to synchronize, and the metric remains low. Finally, if the duration of refractory is appropriately chosen, e.g. ϕ_{refr}=0.25, nodes synchronize, and the metric displays a constant value that is close to r_n=1. The difference $1-r_n$ accounts for the effect of propagation delays, as the achieved accuracy is bounded by these delays.

To generalize these results, Figure 10 plots the achieved mean synchronization index for different maximum propagation delays as the refractory duration ϕ_{refr} augments, where ϕ_{refr} is common to all nodes. Simulations are conducted in networks of N=25 nodes with κ=0.03.

Figure 10 confirms that the stability condition (15) is valid in meshed networks. In case $\phi_{\text{refr}}<2\,\nu_{\max}/T$, the refractory duration is too short, so that the system is unstable, expressed by a low synchronization metric r_n. For

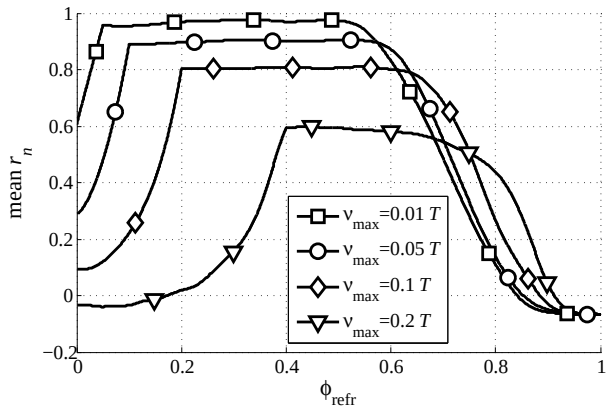

Figure 10: Mean synchronization index for different values of the maximum propagation delay.

$2\,\nu_{\max}/T \leq \phi_{\text{refr}} < 0.5$, the synchronization index is maximum and remains constant. Thus the achieved accuracy does not depend on the refractory duration ϕ_{refr} but only on propagation delays. Finally, when $\phi_{\text{refr}} > 0.5$, the synchronization index drops due to deafness between nodes, i.e. nodes spend more time in refractory than in listen, and when nodes are only in refractory ($\phi_{\text{refr}}=1$), the synchronization metric is minimal, as nodes remain in the initial unordered state.

6. CONCLUSION

This paper studied the model of pulse-coupled oscillator applied to meshed networks. A synchronization metric suitable for locally coupled oscillators was presented, and shown to be useful in studying the synchronization process. To demonstrate how the proposed metric characterizes the synchronization state of the network, two case studies were conducted. The first study looked at the synchronization in the presence of frequency drift, and showed that even in sparsely connected meshed networks, nodes synchronize as long as a maximum drift is observed. The second study extended to meshed networks a stability condition derived for two nodes, and showed that if the refractory period is appropriately chosen, the network synchronizes.

7. REFERENCES

[1] N. L. Biggs. *Algebraic Graph Theory*. Cambridge University Press, 1994.

[2] P. C. Bressloff and S. Coombes. Dynamics of strongly coupled spiking neurons. *Neural Comp.*, 12(1):91–129, Jan. 2000.

[3] P. C. Bressloff, S. Coombes, and B. de Souza. Dynamics of a ring of pulse-coupled oscillators: Group-theoretic approach. *Phys. Rev. Lett.*, 79(15):2791–2794, Oct. 1997.

[4] J. Buck, E. Buck, J. Case, and F. Hanson. Control of flashing in fireflies. V. Pacemaker synchronization in *pteroptyx cribellata*. *J. Comp. Physiology A*, 144(3):630–633, Sep. 1981.

[5] J. Degesys, I. Rose, A. Patel, and R. Nagpal. Desync: Self-organizing desynchronization and TDMA in wireless networks. In *Proc. Conf. on Information Processing in Sensor Networks (IPSN)*, Cambridge, USA, Apr. 2007.

[6] U. Ernst, K. Pawelzik, and T. Geisel. Synchronization induced by temporal delays in pulse-coupled oscillators. *Phys. Rev. Lett.*, 74(9):1570–1573, Feb. 1995.

[7] A. V. M. Herz and J. J. Hopfield. Earthquake cycles and neural reverberations: Collective oscillations in systems with pulse-coupled threshold elements. *Phys. Rev. Lett.*, 75(6):1222–1225, Aug. 1995.

[8] Y.-W. Hong and A. Scaglione. A scalable synchronization protocol for large scale sensor networks and its applications. *IEEE J. Sel. Areas Commun.*, 23(5):1085–1099, May 2005.

[9] E. M. Izhikevich. Weakly pulse-coupled oscillators, FM interactions, synchronization, and oscillatory associative memory. *IEEE Trans. on Neural Networks*, 10(3):508–526, May 1999.

[10] V. Kirk and E. Stone. Effect of a refractory period on the entrainment of pulse-coupled integrate-and-fire oscillators. *Phys. Lett. A*, 232:70–76, Feb. 1997.

[11] Y. Kuramoto. *Chemical Oscillations, Waves, and Turbulence*. Springer-Verlag, 1984.

[12] D. Lucarelli and I.-J. Wang. Decentralized synchronization protocols with nearest neighbor communication. In *Proc. ACM Conf. Embedded Networked Sensor Sys. (SenSys)*, Baltimore, USA, Nov. 2004.

[13] R. Mathar and J. Mattfeldt. Pulse-coupled decentral synchronization. *SIAM J. on Appl. Math.*, 56(4):1094–1106, Aug. 1996.

[14] P. N. McGraw and M. Menzinger. Laplacian spectra as a diagnostic tool for network structure and dynamics. *Phys. Rev. E*, 77(3):031102, 2008.

[15] R. Mirollo and S. Strogatz. Synchronization of pulse-coupled biological oscillators. *SIAM J. on Appl. Math.*, 50(6):1645–1662, Dec. 1990.

[16] C. S. Peskin. *Mathematical Aspects of Heart Physiology*. Courant Institute of Mathematical Sciences, New York University, 1975.

[17] A. Pikovsky, J. Kurths, and M. Rosenblum. *Synchronization: A Universal Concept in Nonlinear Sciences*. Cambridge University Press, 2003.

[18] M. Rhouma and H. Frigui. Self-organization of pulse-coupled oscillators with application to clustering. *IEEE Trans. on Pattern Analysis and Machine Intelligence*, 23(2):180–195, Feb. 2001.

[19] S. Strogatz. *Sync: How Order Emerges from Chaos in the Universe, Nature, and Daily Life*. Hyperion, 2004.

[20] A. Tyrrell, G. Auer, and C. Bettstetter. Fireflies as role models for synchronization in wireless networks. In *Proc. Int. Conf. Bio-Insp. Models of Network, Info. and Comp. Sys. (BIONETICS)*, Cavalese, Italy, Dec. 2006.

[21] G. Werner-Allen, G. Tewari, A. Patel, M. Welsh, and R. Nagpal. Firefly-inspired sensor network synchronicity with realistic radio effects. In *Proc. ACM Conf. Embedded Networked Sensor Sys. (SenSys)*, San Diego, USA, Nov. 2005.